ARTICLE

Zengqian Hou · Pusheng Zeng · Yongfeng Gao · Andao Du · Deming Fu

Himalayan Cu–Mo–Au mineralization in the eastern Indo–Asian collision zone: constraints from Re–Os dating of molybdenite

Abstract We present new Re–Os molybdenite age data on three porphyry Cu–Mo–Au deposits (Yulong, Machangqing, and Xifanping). These deposits are associated with the Himalayan adakitic magmatism that occurred in a continental collision environment, controlled by large-scale Cenozoic strike-slip faults in the eastern Indo–Asian collision zone. Three distinct episodes of Cu–Mo–Au mineralization are recognized. At Yulong, Re–Os isotopic data of four molybdenite samples from sulfide-quartz veins in the quartz–sericite alteration zone yield an isochron with an age of 40.1 ± 1.8 Ma (2σ), coincident to a zircon sensitive high-mass resolution ion microprobe (SHRIMP) age of 40.9 ± 0.1 Ma for the host monzogranite. The molybdenite Re–Os dates, together with K–Ar, Rb–Sr, U–Pb, and $^{40}Ar/^{39}Ar$ dates on the pre- and intra-ore porphyries, suggest that Cu–Mo–Au mineralization formed during the late stage (~40 Ma) of regional porphyry magmatism, but hydrothermal activity probably lasted to at least ~36 Ma. At Machangqing, molybdenite Re–Os data from the K–silicate and quartz–sericite alteration zones yield an isochron with an age of 35.8 ± 1.6 Ma (2σ), which is identical to the zircon SHRIMP and bulk-rock Rb–Sr ages (35~36 Ma) of the host granite, but older than bulk-rock K–Ar dates (31~32 Ma) for associated Au-bearing quartz syenite with advanced argillic alteration. At Xifanping, five molybdenite samples from the K–silicate alteration zone yield the youngest Re–Os isochron age in the area, at 32.1 ± 1.6 Ma (2σ). The Re–Os molybdenite dates here are younger than K–Ar ages (33.5~34.6) for hydrothermal biotite and actinolite. There is a positive correlation between the absolute age of the deposits and their Cu and Au reserves in the eastern Indo–Asian collisional zone. Episodic stress relaxation probably caused multiple magmatic intrusions, which most likely resulted in three episodes of Cu–Mo–Au mineralization in the eastern Indo–Asian collision zone.

Keywords Re–Os isotopes · Porphyry Cu–Mo–Au deposits · Eastern Indo–Asian collision zone · Himalayan · Tibet

Editorial handling: G. Beaudoin

Z. Hou (✉) · P. Zeng
Institute of Mineral Resources,
Chinese Academy of Geological Sciences,
26 Baiwanzhuang Road,
Beijing, 100037, People's Republic of China
e-mail: houzengqian@126.com
Tel.: +81-883-64366
Fax: +81-683-17264

Y. Gao
Department of Geology,
Shijiazhuang Economic College,
Hebei, 05000, People's Republic of China

A. Du
National Research Center of Geoanalysis,
Chinese Academy of Geological Sciences,
Beijing, 100037, People's Republic of China

D. Fu
Sichuan Bureau of Geology and Mineral Resources,
Chengdu, 61000, People's Republic of China

Introduction

The eastern Indo–Asian collision zone is located along the eastern margin of the Tibetan plateau, and is bounded by a series of north- and northwest-striking Cenozoic faults (Fig. 1a, Wang J-H et al. 2001). The collision zone is a significant porphyry-type Cu–Mo–Au province in China, and has much economic potential. The mineralization in the collision zone is associated with Cenozoic alkali-rich magmatic rocks, which were controlled by large-scale strike-slip faults roughly orthogonal to convergence between the Indian and Asian continents (Hou et al. 2003). The mineralization occurs in two sub-parallel porphyry Cu–Mo–Au belts (Fig. 1a, Hou et al. 2004a). Within both belts, a number of economic porphyry Cu, Cu–Mo, Cu–Au, and Au deposits were discovered (Table 1). The geology and genesis of these deposits were investigated by many researchers (Rui et al. 1984; Ma 1990; Cai
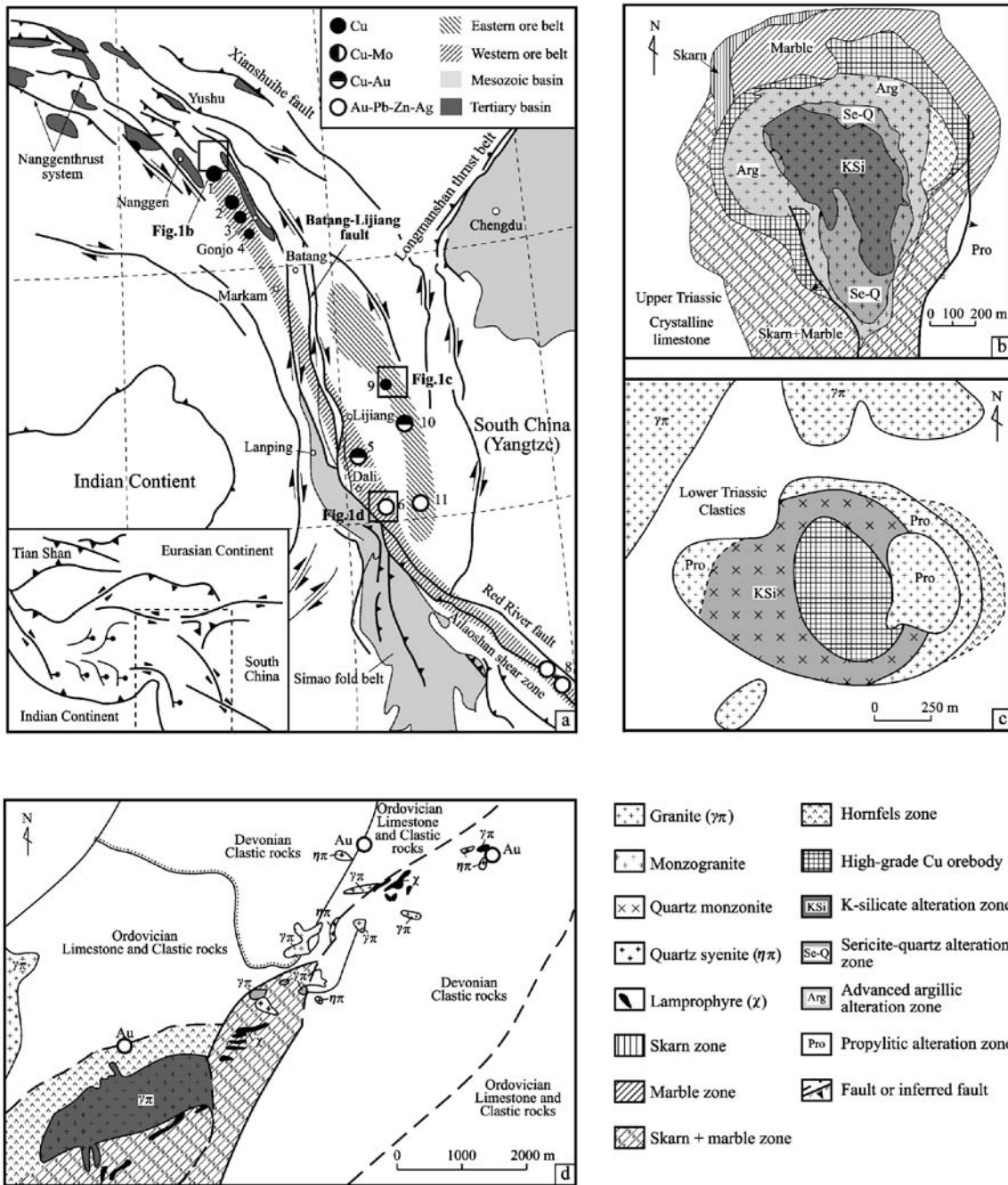
Fig. 1 a Simplified geologic map showing the Cenozoic tectonic framework and the distribution of porphyry Cu–Mo–Au deposits in the eastern Indo–Asian collision zone (modified from Wang J-H et al. 2001; Hou et al. 2003); ore deposits: *1* Yulong, *2* Douxiasong-duo, *3* Malasongdou, *4* Mamupu, *5* Beiya, *6* Machangqing, *7* Habo, *8* Chang'an, *9* Xifanping, *10* Bainiuchang, *11* Yao'an. **b–d** Simplified maps showing the alteration zonation and mineralization in the Yulong (**b**, after Hou et al. 2003), Xifanping (**c**, Wang et al. 2002) and Machangqing deposits (**d**, Huang et al. 1996)

1992; Tang and Luo 1995; Huang et al. 1996; Xu et al. 1997; Peng et al. 1998; Hou et al. 2003; Ge et al. 2003), but the metallogenic evolution of the collision zone is poorly understood. This ~1,000-km-long magmatic belt in the collision zone has an age range of 55~17 Ma (Zhang and Xie 1997; Luo et al. 1998; Wang et al. 2002; Hou et al. 2003), but the ages of units that host economic mineralization is not well constrained. To better understand the porphyry Cu–Mo–Au systems in the collision zone,

accurate determination of the age and duration of the Cu–Mo–Au mineralization have become a focus of much interest.

The age of mineralization was previously inferred from U–Pb zircon, Rb–Sr isochron, and K–Ar dates for pre- and intra-mineralized intrusive rocks (Liu et al. 1981; Chen 1983; Ma 1990; Tang and Luo 1995; Hou et al. 2003), and $^{40}Ar/^{39}Ar$ and K–Ar dates for hydrothermal minerals (biotite, sericite, actinolite) (Fu 1996; Xu et al.

Table 1 Summary of geological and mineralogical features of the porphyry Cu–Mo–Au deposits in the eastern Indo–Asian collision zone

Deposit	Wall rock	Rock type	Alteration	Grade and tonnage	Shape of orebody	Ore structure	Sulfide assemblages	Economic metals
Eastern porphyry copper belt								
Yulong[a]	T_3; crystalline limestone	Monzogranite, quartz monzonite	K-silicate, quartz–sericite, propylitic, skarn	6.22 Mt Cu Cu: 0.99% Mo: 0.028 Au: 0.35 ppm	Stratiform and lenticular orebody surrounding stock, pipe-like orebody	Veinlet, disseminated, brecciated	Cp+Mo+Py; Co+Cc+Py±Te ±G±S±Wo`	Cu±Mp±Au ±Ag±Pt±Co
Malasongduo[a]	T_1; rhyolitic rocks	Monzogranite, granite	K-silicate, quartz–sericite, propylitic, skarn	1.0 Mt Cu Cu: 0.44% Mo: 0.14% Au: 0.06 ppm	Regular lenticular orebody in stock	Veinlet, disseminated, pervasive	Cp+Py+Mo+Ga +Sp±Bo±Te	Cu±Mo±Au ±Ag±Pt±Pd
Duoxiasongduo[a]	T_3; sandy mudstone	Monzogranite, alkali-feldspar granite	K-silicate, quartz–sericite, propylitic, skarn	0.5 Mt Cu Cu: 0.38% Mo: 0.04% Au: 0.06 ppm	Regular lenticular orebody in stock	Veinlet, disseminated, stockwork	Cp+Py+Mo+Mt ±Ga±Sp±Bo	Cu±Mo±Ag
Mangzong[a]	T_3; sandy mudstone	Monzogranite	K-silicate, quartz–sericite, propylitic, skarn	0.25 Mt Cu Cu: 0.34% Mo: 0.03% Au: 0.02 ppm	Regular pipe-like orebody in stock	Veinlet, disseminated	Cp+Py+Mo±Ga ±Sp±Cc±Te	Cu±Mo±Au
Zhanaga[a]	T_3; sandy mudstone	Monzogranite, alkali-feldspar	K-silicate, quartz–sericite, propylitic, skarn	0.3 Mt Cu Cu: 0.36%	Pipe-like orebody in stock	Veinlet, disseminated	Cp+Mo+Py ±Mt±Cc±Bo	Cu±Mo±Au
Machangqing[b]	O_1–D_1; limestone and sandstone	Granite, monzogranite, quartz syenite	K-silicate, sericite, advanced argillic, skarn	0.25 Mt Cu Cu: 0.08% Mo: 0.08% Au: 0.35 ppm	Lenticular, pocket, and irregular orebodies in stock	Veinlet, disseminated, massive	Cp+Py+MtHm+G +PyAr±Sp+Ga	Cu±Mo; Au±Cu
Beiya[b]	P_2; basalts, T_2; limestone, dolomite and clastic rock	Quartz syenite, lamprophyre	K-silicate, sericite, chloritization, skarn	27 t Au Au: 4.93 ppm Cu: 0.36%	Veinlet, lenticular, and stratiform orebodies in stock	Banded, veinlet, disseminated	G+Cp+Mt+Py±Hm	Au±Cu±Fe ±Ag±Pb±Zn
Habo[c]	T: sandstone, S_1: sandstone, siltstone and slate	Quartz syenite, granite, lamprophyre	K-silicate, sericite, carbonization, skarn	20 t Au Au: 5.02 ppm	Lenticular orebody in skarn; vein in porphyry stock	Vein/veinlet, dissemination	G+Cp+Py+Bo ±Ga±Sp	Au±Cu±Ag ±Pb±Zn
Chang'an[d]	Paleozoic breccia sandstone, and limestone	Syenite, quartz syenite, granite porphyry	K-silicte, sericite, kaolinization, skarn	34.1 t Au Au: 6.0 ppm Mo: 0.122% Cu: 1.5%	Veinlet hosted in wall rock	Disseminated, veinlet, brecciated	G+Cp+Py+Mt +Sp+Ga+Mo	Au+Cu+Mo +Ag±Pb±Zn

Table 1 (continued)

Deposit	Wall rock	Rock type	Alteration	Grade and tonnage	Shape of orebody	Ore structure	Sulfide assemblages	Economic metals
Xifanping[e]	T₁: sandstone; P₂: clastic rock and mudstone	Quartz monzonite	K-silicate, sericite, propylitic, phyllitic	0.18 Mt Cu Cu: 0.28% Au: 0.31 ppm	Lenticular orebody hosted in stock	Veinlet, disseminated	Py+Cp+Ga±Mo ±Sp±Mt±G	Cu±Au±Mo
Yao'an[f]	Cretaceous sandstone and mudstone	Quartz syenite, quartz monzonite, lamprophyre	K-silicate, sericite, baritization, carbonitization, kaolinitization	>2 t Au Au: 0.6~44 ppm	Vein hosted in lamprophyre and quartz syenitic stock	Brecciated, veintlet	G+Py+Spe+Lim +Sp+Ga+Arg+Mt	Au±Ag±Pb±Zn

Py Pyrite, *Cp* Chalcopyrite, *Mo* Molybdenite, *Co* Covellite, *Cc* Chalcocite, *Ar* Arsenopyrite, *Ga* Galena, *Sp* Sphalerite, *Pr* Pyrrhotite, *Mt* Magnetite, *Spe* Specularite, *Lim* Limonite, *Arg* Argentinite, *Bo* Bornite, *Hm* Hematite, *Te* Tetrahedrite, *G* Gold, *S* Silver, *Wo* W-bearing minerals
Data sources: ᵃRui et al. (1984), Tang and Luo (1995), and Hou et al. (2003); ᵇHuang et al. (1996), and Peng et al. (1998); ᶜCai (1992); ᵈMo et al. (1993); ᵉXu et al. (1997), Luo et al. (1998); ᶠGe et al. (2003)

1997; Luo et al. 1998; Wang D-H et al. 2001). However, the ages of host rocks and ore-associated minerals do not necessarily agree with the actual mineralization age in many cases. This disparity is particularly apparent for K–Ar and ⁴⁰Ar/³⁹Ar dates on presumed ore-associated minerals (Ishihara et al. 1989; Suzuki et al. 1996). Moreover, the mineralized stocks in many ore districts are usually complex and multiple, and mineralization is commonly formed during multiple episodes (Tang and Luo 1995; Luo et al. 1998; Wang D-H et al. 2001; Hou et al. 2003).

Recent studies have documented that the Re–Os system in molybdenite can yield the accurate age of sulfide mineralization, and allows an estimation of the duration of sulfide mineralization in hydrothermal systems and metallogenic provinces (Luck and Allègre 1982; McCandless et al. 1993; Stein et al. 1997, 1998; Selby and Creaser 2001; Selby et al. 2002; Barra et al. 2003; Hou et al. 2004b). To aid in defining the metallogenic history of the study area, we investigated the Yulong, Machangqing and Xifanping deposits, which are representative of porphyry-type mineralization in terms of typical host lithologies, sulfide assemblage, alteration zonation, and economic metals (Table 1). This paper provides precise Re–Os dates from molybdenite, defines three episodes of mineralization, and discusses the metallogenic history and hydrothermal duration of porphyry ore systems in the eastern Indo–Asian collision zone.

Geology

The Tertiary geology of east Tibet is characterized by a series of north- and northwest-striking Cenozoic faults, with a large Cenozoic alkali-rich igneous belt and associated Tertiary basins in the eastern Indo–Asian collision zone (Fig. 1a). The collision zone is also a tectonic transform zone that has accommodated and adjusted to the collisional strain of Indo–Asian convergence since the Paleocene. The Cenozoic deformation in the collision zone is chiefly manifested by Eocene–Oligocene (40~24 Ma) transpressional deformation, early–middle Miocene (24~17 Ma) transtensional deformation, and east–west extension since the Neogene (Wang J-H et al. 2001). Strike-slip fault systems include from west to east: the Jiali and Gaoligong faults around the eastern Himalayan syntaxis, the Batang–Lijiang fault (northern segment) and the Ailaoshan–Red River fault (southern segment), and the Xianshuihe and Xiaojiang faults in the Yangtze craton (Fig. 1a). Both Cenozoic alkali-rich igneous rocks and a series of early–middle Cenozoic pull-apart basins developed along a narrow belt following the Nanqian thrust, the Batang–Lijiang fault, and the Red River shear zone, forming a 1,000-km-long alkali-rich magmatic belt (Zhang et al. 1998a,b). This belt can be divided into two ore-bearing potassic porphyry sub-belts (Fig. 1a, Hou et al. 2004a). The western Jomda–Heqing–Dali sub-belt is distributed along the Batang–Lijiang fault in the western margin of the Yangtze craton, whereas the

eastern Yanyuan–Yao'an sub-belt occurs within the Yangtze craton (Fig. 1a). Dating indicates that the igneous rocks in the western sub-belt have ages ranging from 55 to 17 Ma (Zhang and Xie 1997), whereas those in the eastern sub-belt have ages ranging from 48 to 24 Ma (Luo et al. 1998). Main porphyry phases are monzonitic, quartz monzonitic, monzogranitic, K-feldspar granitic, and quartz syenitic and syenitic. In general, monzogranitic and K-feldspar granitic porphyries are associated with Cu–Mo and Cu–Au mineralization, whereas quartz syenite mainly hosts porphyry Au mineralization. Geochemical studies indicate that Cu–Mo–Au-bearing porphyritic rocks show magmatic affinity with adakite (Hou et al. 2004a), but are characterized by high alkali and K_2O contents, different from typical Na-rich adakite (Defant and Drummond 1990; Kay et al. 1993; Drummond et al. 1996). In contrast, barren syenitic porphyritic rocks are characterized by low SiO_2 contents (<63 wt.%), with high Ba and Y abundances (Hou et al. 2004a).

Porphyry copper–molybdenum–gold mineralization

Two sub-parallel porphyry Cu–Mo–Au belts appear in the Indo–Asian collision zone (Fig. 1a). The northern segment of the western belt comprises the Yulong porphyry Cu deposit, whereas the Beiya Au–Cu ore field and the Machangqing Cu–Mo–Au deposit are in the central segment, and the Chang'an and Habo Au deposits occur in the southern segment (Fig. 1a). The eastern belt comprises the Xifanping Cu–Au, Bainiuchang Cu, and Yao'an Au–Ag (±Pb±Zn) deposits (Fig. 1a). Ore-bearing porphyries in both Cu–Mo–Au belts show similar petrographic and geochemical features, but yield distinct $^{260}Pb/^{204}Pb$ ratios (18.576~18.908 in the western belt vs 18.078~18.205 in the eastern belt; Hou et al. 2004a). These ore-bearing porphyry intrusions typically intrude Paleozoic and Mesozoic sedimentary sequences, and mostly occur as small stocks (Fig. 1). They are generally multiphase and complex, and associated mineralization occurs preferentially in the latest phase of porphyry systems. The geologic and mineralogical features of these deposits are listed in Table 1, and three representative deposits are briefly described here.

Yulong

The Yulong copper deposit is the largest (630 Mt) in the Yulong belt. It has reserves of over 6.22 Mt of contained copper and an average grade of 0.99% Cu, 0.028% Mo, and 0.35 ppm Au (Table 1). It is composed of a ring-shaped high-grade Cu–Au zone (~3 Mt Cu, at >1% Cu; ~100 t Au, at 4 ppm Au; Tang and Luo 1995) overlying or/and surrounding a pipe-like, steeply dipping, veinlet-disseminated Cu–Mo orebody within the monzogranite stock (Fig. 1b). Early alteration, associated with porphyry Cu–Mo mineralization, produced concentric alteration zones ranging from an inner K-silicate zone through a quartz–sericite zone to an outer propylitic zone (Fig. 1b). Hydrothermal

fluids are characterized by high temperature (300~600°C), and high salinity (23~54 wt.% NaCl), $\delta^{18}O$=0.0~7.4‰ and δD=−102~−65‰ (Li et al. 1981; Tang and Luo 1995; Hou et al. 2005). The late alteration is characterized by structurally controlled advanced argillic assemblages of quartz, kaolinite, dickite, endellite, montmorillonite, hydromica, and minor alunite, which overprinted early-formed alteration halos and replaced subhorizontal or outward-dipping hydrothermal breccias near the roof of the stock (Hou et al. 2005). Associated Cu–Au mineralization formed sulfide assemblages consisting of hypogene chalcocite, covellite, tennantite, pyrite, and minor chalcopyrite, which comprise the major part of the high-grade Cu zone (Hou et al. 2005). Fluid inclusion and $\delta^{18}O–\delta D$ data indicate that this late-stage fluid is a CO_2-rich, low-temperature (115~345°C), low-salinity (3~12 wt.% NaCl), acidic fluid, dominated by meteoric water with a small proportion of magmatic water (Rui et al. 1984).

Machangqing

The Machangqing deposit in the western belt is a typical Cu–Mo deposit, with reserves of 39 Mt of Cu ore (at 0.64% Cu) and 56 Mt of Mo ore (at 0.08% Mo). The mineralization is associated with Himalayan granitic stocks, which intruded an Ordovician sedimentary sequence. The ores occur as Cu–Mo veinlets within the stock that underwent K-silicate, phyllic, and argillic alteration, and as Cu–Mo skarns developed between the stock and limestone. About 0.2~1.0-cm-wide veinlets are mainly composed of intermediate-fine-grained quartz and sulfide assemblages of molybdenite, pyrite, and chalcopyrite. Molybdenite is disseminated as small flakes (0.02×0.2 mm in size) with a modal abundance of 1 to 3 vol% in or along the inner edges of quartz veinlets (Peng et al. 1998). Molybdenite also occurs in small veins and as disseminations in altered rock. Fluid inclusion studies indicate that early-stage fluids for Cu–Mo skarn mineralization have homogenization temperatures ranging from 300 to 500°C, and salinities of 10.2~42.0 wt.% NaCl eq., whereas the main stage fluids that produced the Cu–Mo veinlets have lower temperatures (210~350°C) and lower salinities (5.0~14.6 wt.% NaCl eq.) (Yang and Tang 1996; Peng et al. 1998).

There are two distinct episodes of gold mineralization at Machangqing. Early Au mineralization together with Cu is associated with magnetite-rich K-silicate alteration. The late Au mineralization is hosted in quartz syenite emplaced along fracture zones, and is associated with texture-destructive advanced argillic alteration. Gold orebodies (~12 t Au) partly overprint porphyry Cu–Mo mineralization, and are mainly developed in fractured clastic rocks (Fig. 1d; Ge et al. 2003). Gold occurs in Au-bearing quartz veins and as disseminations in rocks altered by silicification. Au-bearing sulfide assemblages consist of arsenopyrite, pyrite, sphalerite, galena, and minor chalcopyrite. Fluid inclusions of the gangue quartz define a range of temperature from 132 to 255°C (Yang and Tang 1996).

Xifanping

The Xifanping deposit represents porphyry Cu–Au mineralization with 0.18 Mt Cu (at 0.28% Cu; at 0.31 ppm Au) in the eastern belt. The mineralization is associated with a multistage quartz monzonite stock, intruding a Permo–Triassic clastic sequence. The Cu–Mo orebodies, dominated by veinlet-disseminated pyrite–chalcopyrite–magnetite–native gold±molybdenite±galena±sphalerite, occur within the stock and near the contact between the stock and clastic host rocks. Early-formed quartz vein and stockwork ores have more molybdenite and are associated with K-silicate alteration assemblages, whereas the later veinlet and disseminated ores have minor molybdenite, and are associated with propylitic alteration assemblages dominated by chlorite and calcite (Fig. 1d). Gold mineralization occurs in the K-silicate alteration halo characterized by up to 15% of

magnetite. Hydrothermal fluids associated with Cu–Au mineralization are characterized by high temperature (350~620°C) and high salinity (39.7~66.5 wt.% NaCl eq.) (Xu et al. 1997). The fluid $\delta^{18}O$ values range from 7.5~8.3‰ in K-silicate alteration to 4.2~4.4‰ in the propylitic zone, suggesting the evolution of ore fluids from magmatic to meteoric water (Xu et al. 1997).

Sample description and analytical method

Twenty-two molybdenite samples were obtained by crushing the ore samples in a porcelain disk mill, and separating molybdenite by heavy liquid techniques. The molybdenite samples were handpicked under a microscope to remove all impurities. The Yulong samples (Y-54, -56, -57, and -58) were collected from a 2-cm-thick quartz vein with molybde-

Table 2 Re–Os isotopic data for molybdenites from five typical porphyry Cu–Mo–Au deposits in the eastern Indo–Asian collision zone

Sample no.	Occurrence	Mineral assemblage	Total Re (ppm)	187Re (ppm)	187Os (ppb)	Re–Os model age
Xifanping Cu–Au deposit						
ZK004-153	Sulfide veinlet disseminated orebody	Qtz+Py+Cp+Mo	117.3 (1.2)	73.7 (0.7)	40.1 (0.5)	33.1 (0.6)
ZK004-165		Qtz+Py+Cp+Mo	220.8 (3.0)	138.8 (1.9)	73.1 (0.7)	31.6 (0.6)
ZK004-174		Py+Cp+Mo+Qtz+Kf	9.4 (0.1)	5.9 (0.1)	3.6 (0.1)	36.2 (1.3)
ZK005-305		Qtz+Py+Cp±Mo	88.4 (0.8)	55.5 (0.5)	30.8 (0.4)	33.3 (0.6)
ZK007-150		Qtz+Py+Cp+Mo	380.5 (6.6)	239.1 (4.1)	124.4 (1.0)	31.2 (0.7)
Weighted mean						33.1±0.8
Isochron age					5 points	32.1±1.6
Machangqing Cu–Mo–Au deposit						
MCQ-1	Sulfide-quartz veins, sulfide veinlet,	Mo+Py+Ch+Qtz	66.0 (0.6)	41.5 (0.4)	24.3 (0.2)	35.1 (0.5)
MCQ-2	disseminated orebody	Mo+Py+Kf+Qtz	89.6 (1.0)	56.3 (0.6)	34.4 (0.4)	36.6 (0.6)
MCQ-4-1		Mo+Py+Ch+Qtz	84.5 (1.0)	53.1 (0.6)	32.0 (0.3)	36.1 (0.6)
MCQ-4-2		Mo+Py+Ch+Qtz	84.7 (0.8)	53.2 (0.5)	32.5 (0.3)	36.7 (0.6)
MCQ-5-1		Mo+Qtz+Ser	30.5 (0.3)	19.2 (0.2)	11.3 (0.1)	35.5 (0.6)
MCQ-5-3		Mo+Qtz+Ser	33.6 (0.3)	21.1 (0.2)	12.3 (0.1)	34.9 (0.6)
MCQ-20-1		Mo+Py+Cp+Qtz	123.3 (1.2)	77.5 (0.8)	44.7 (0.4)	34.6 (0.6)
MCQ-20-2		Mo+Py+Cp+Qtz	125.1 (1.4)	78.6 (0.9)	45.4 (0.4)	34.7 (0.6)
Weighted mean						35.6±0.6
Isochron age					8 points	35.8±1.6
Yulong Cu deposit						
Y-54	Quartz veins in quartz -sericite	Py+Cp+Mo+Qtz	387.0 (4.3)	243.3 (2.7)	164.3 (1.5)	40.5 (0.7)
Y-56	alteration zone	Py+Cp+Mo+Qtz	664.5 (7.2)	417.7 (4.5)	281.3 (2.1)	40.4 (0.7)
Y-57		Py+Cp+Mo+Qtz	290.5 (3.5)	182.6 (2.2)	124.7 (1.0)	41.0 (0.8)
Y-58		Py+Cp+Mo+Qtz	433.0 (6.3)	272.1 (4.0)	185.5 (1.9)	40.9 (0.7)
Weighted mean						40.7±0.7
Isochron age					4 points	40.1±1.8
Malasongduo Cu deposit						
Ma-1[a]	Quartz veins in K-silicate zone	Cp+Mo+Py+Qtz				35.8±0.4
Duoxiasongduo Cu deposit						
Du-1[a]	Quartz veins in K-silicate zone	Cp+Py+Mo+Qtz				36.0±0.4

Values in parenthesis are absolute uncertainties (2σ). Uncertainties in ages are calculated using error propagation and include errors in the 185Re and 190Os spike calibration, the Re decay constant, and spectroscopic measurements. Model age and isochron age were calculated using Isoplot (Ludwig 2001). Uncertainties for ages are absolute (2σ)
Py pyrite, *Cp* chalcopyrite, *Mo* molybdenite, *Qtz* quartz, *Kf* K-feldspar, *Ser* sericite, *Ch* chlorite
[a]Data source: Du et al. (1994)

nite, pyrite, and minor chalcopyrite, occurring in the quartz–sericite alteration zones. Samples at Machangqing were collected from a molybdenite veinlet (MCQ-1, -4) and a sulfide-quartz vein (MCQ-5) crosscutting the host porphyritic granite, and two samples are from disseminated ore with molybdenite, pyrite, and chalcopyrite (MCQ-2, -20). Samples at Xifanping were collected from three separate drill cores, which intersect the main orebody with a quartz–pyrite–chalcopyrite–molybdenite assemblage. Sample ZK004-174 is from disseminated sulfides; the other samples are from sulfide-quartz veinlets hosted in the K-silicate alteration halo. All molybdenite concentrates were milled to powder, and then, to avoid possible Re contamination, the concentrates were screened by microprobe to make sure that there was no clay intergrowth in the analyzed molybdenite (McCandless et al. 1993).

The ^{187}Re and ^{187}Os concentrations in 0.02~0.05 g molybdenite aliquots were determined using a TJA Plasmaquad ExCell inductively coupled plasma-mass spectrometry (ICP-MS) at the Re–Os Lab, National Research Center of Geoanalysis (Beijing). The Carius tube method was used for the dissolution of molybdenite and equilibration of samples and tracer ^{185}Re and ^{190}Os at 230°C for 1 h (Du et al. 1994; Shirey and Walker 1995; Smoliar et al. 1996). Upon cooling, the bottom part of the tube was frozen, the neck of the tube was broken, and the contents of the tube were poured into a distillation flask and the residue was washed out with 40 ml of water. Os was distilled twice. In the first distillation step, OsO_4 was distilled at 105~110°C for 50 min, and was trapped in 10 ml of water. The residual Re-bearing solution was saved in a 50 ml beaker for Re separation. The water trap solution, plus 40 ml of water, was distilled a second time. The OsO_4 was distilled for 1 h and trapped in 10 ml of water for the determination of the Os isotope ratio.

The Re-bearing solution was evaporated to dryness; 1 ml of water was added, and then the solution was heated to near-dryness twice. Ten milliliters of 20% NaOH was added to the residue, followed by Re extraction with 10 ml of acetone in a 120-ml Teflon separation funnel. After discarding the water from the residue and washing it in acetone with 2 ml of 20% NaOH, the acetone was transferred into a 100-ml beaker that contained 2 ml of water, evaporated to dryness, and picked up in 2% HNO_3 for determination of the Re isotope ratio. If the concentration of the Re-bearing solution was more than 1 mg/ml, the Na was removed using cation-exchange resin (Du et al. 1994).

Average blanks for the total Carius tube procedure are 10 pg Re and 1 pg Os. The analytical reproducibility was tested by repeated analyses of molybdenite standard HLP-5 from a carbonatite vein-type molybdenum–uranium deposit in the Jinduicheng–Huanglongpu area of the Shaanxi province, China. Seventeen samples were analyzed over a period of 6 months. The uncertainty in each individual age determination is about 1.35%, including the uncertainty of the decay constant of ^{187}Re, uncertainty in isotope ratio measurement, spike calibrations, and spike weighing errors. The average Re–Os age on HLP-5 is 221.3±0.3 Ma (95% confidence level). Median age and mean absolute

deviation is 221.3±0.12 Ma. The average Re concentration is 283.71±1.54 μg/g. The average Os concentration is 657.95±4.74 ng/g. Our HLP-5 age and Os and Re contents are in agreement with results reported in the literature (Stein et al. 1997; Selby and Creaser 2001).
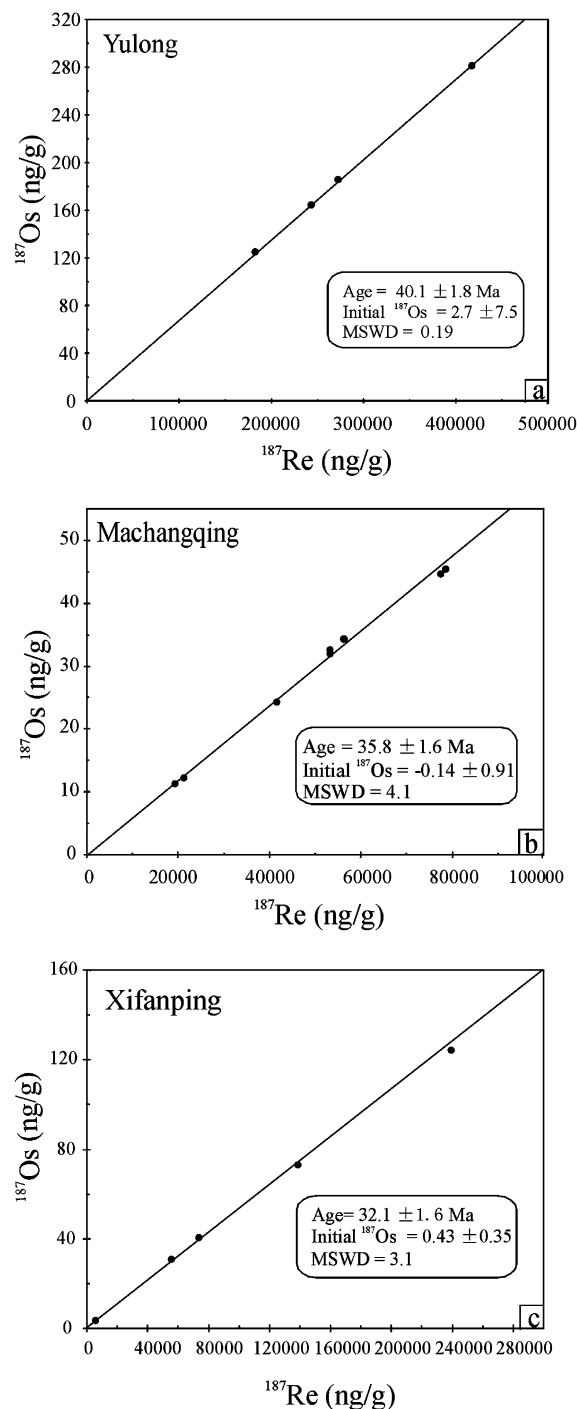

Fig. 2 Molybdenite ^{187}Re–^{187}Os isochrones for three porphyry Cu–Mo–Au deposits in the eastern Indo–Asian collision zone. The isoplot of Ludwig (2001) was used for the isochron determinations. The symbol size is greater than uncertainty for ^{187}Re and ^{187}Os

Table 3 Summary of age data of the pre-, intra-, and post-ore intrusives and associated hydrothermal alteration minerals

Area	Intrusion	Rock type	Economic metal	Analyzed phase	Method	Age (Ma)	Reference
Pre- and intra-ore intrusives							
Yulong porphyry Cu belt	Yulong	Quartz monzonite		Bi; WR	Ar/Ar;K–Ar; Rb/Sr	52.0–55.0 (5)	Hou et al. (2003); Liang (2002);
		Monzogranite	Cu±Mo	Bi, Kf; WR	K–Ar; Rb–Sr	37.9–41.5 (9)	Tang and Luo (1995); Ma (1990);
		Monzogranite	Cu±Mo	Zr	SHRIMP	40.9±0.1	Chen (1983);
	Malasongduo	Monzogranite		WR	K–Ar	50.9	Liu et al. (1981)
		Monzogranite		Zr	U–Pb	40.9	
		Monzogranite	Cu±Mo	Zr	SHRIMP	37.1±0.2	
		Granite		Zr	U–Pb	33.7	
	Duoxiasongduo	Monzogranite		WR	Rb–Sr	52.0	
		Monzogranite		Zr	U–Pb	41.0	
		Monzogranite	Cu±Mo	Zr	SHRIMP	37.5±0.2	
		Alkali-feldspar granite		Kf	K–Ar	32.4	
	Zhanaga	Monzogranite		Kf	K–Ar	40.0	
		Monzogranite		Zr	SHRIMP	38.5±0.2	
		Alkali-feldspar granite	Cu±Mo	Bi, Kf	K–Ar	33.9–35.9 (4)	
	Mangzong	Monzogranite		Kf	K–Ar	41.0	
		Monzogranite		Zr	SHRIMP	37.6±0.2	
		Monzogranite	Cu±Mo	Kf	K–Ar	30.9–33.9(2)	
Beiya Ore-field	Hongnitang	Quartz syenite		WR	K–Ar	47.75±1.07	Wang D-H et al. (2001)
	Hongnitang	Quartz syenite	Au±Cu	Kf	K–Ar	37.50±1.36	
	Wandongshan	Quartz syenite	Au±Cu	WR	K–Ar	35.98±1.43	
	Wulipan	Quartz syenite	Au±Cu	WR	K–Ar	38.36±0.57	
Xiangyun	Machangqing	Granite		??	K–Ar	48.0	Fu (1996)
		Granite	Cu–Mo±Au	??	Rb–Sr	36.0	Luo et al. (1998)
		Granite	Cu–Mo±Au	Zr	SHRIMP	35.0±0.2	Liang (2002)
		Quartz syenite	Au	WR	Rb–Sr	34.0	Fu (1996)
Yuanyang	Habo	Quartz syenite	Au	WR	Rb–Sr	37.5	Luo et al. (1998)
Jinping	Chang'an	Amphibole syenite		Bi	K–Ar	36.0	Fu (1996)
Yanyuan	Xifanping	Quartz monzonite		Kf	K–Ar	51.9	Luo et al. (1998)
		Quartz monzonite		Am.	^{40}Ar/^{39}Ar	47.5	Fu (1996)
Heqing	Luobodi	Syenite		WR	Rb–Sr	52.76±11.3	Luo et al. (1998)
		Quartz syenite	Cu–Au	WR	K–Ar	32.37±0.58	Wang D-H et al. (2001)
Altered host rocks and hydrothermal minerals							
Beiya	Bijiashan	Altered quartz syenite	Au±Cu	Ser	K–Ar	37.8±1.3	Wang D-H et al. (2001)
Xiangyun	Machangqing	Altered quartz syenite	Au	WR	K–Ar	31.0–32.0 (2)	Fu (1996)
Jinping	Chang'an	Altered syenogranite	Au	WR	K–Ar	36.0	Luo et al. (1998)
Yanyuan	Xifanping	Altered monzonite	Cu–Au	Bi	K–Ar	34.6	Xu et al. (1997)
		Altered monzonite	Cu–Au	Ac	K–Ar	33.5	
Yao'an	Laojiezi	Altered quartz syenite	Au±Ag	Bi	K–Ar	35.0	Luo et al. (1998)
	Baimazui	Altered quartz syenite	Au±Ag	Bi	K–Ar	31.0	
Post-ore intrusives							
Yulong belt	Yulong	Alkali feldspar granite		Kf	K–Ar	16.5	Tang and Luo (1995)
	Duoxiasongduo	Alkali feldspar granite		Kf	K–Ar	27.8	
	Mangzong	Alkali feldspar granite		Kf	K–Ar	26.4	
Beiya	Hongnitang	Syenite		Plag	^{40}Ar/^{39}Ar	24.82±0.04	Wang D-H et al. (2001)
	Wandongshan	Syenite		Ser	K–Ar	27.76±0.60	
Heqing	Luobodi	Syenite		Plag	^{40}Ar/^{39}Ar	23.82±0.03	Wang D-H et al. (2001)

Kf K-feldspar, *Bi* biotite, *Plag* plagioclase, *Ser* sericite, *Am* amphibole, *Zr* zircon, *WR* whole rock. The numbers in parenthesis are the numbers of analyzed samples
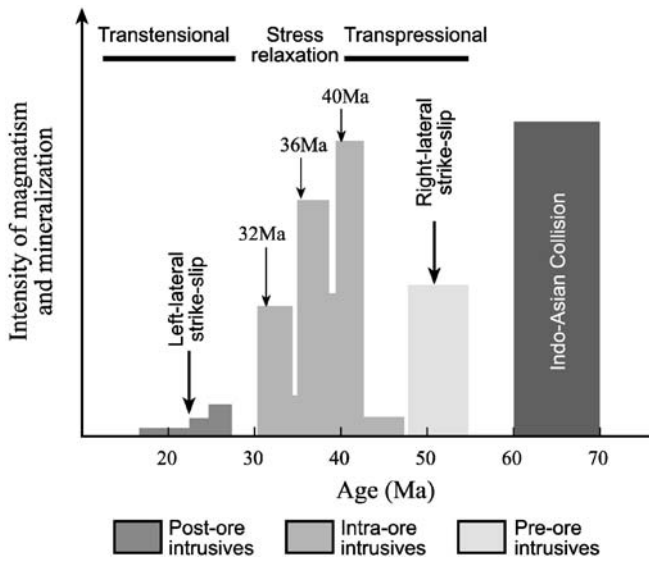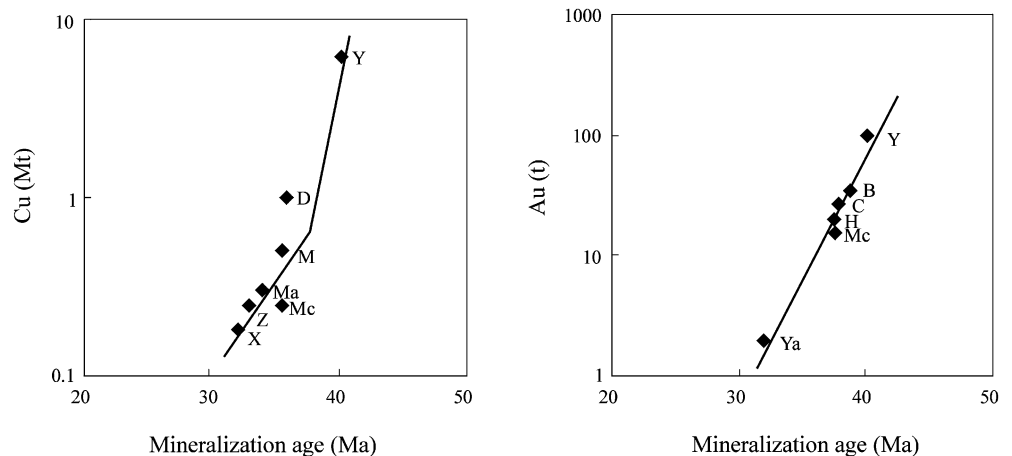
Fig. 3 The relationship of three episodic mineralization events with the stress regimes in the eastern Indo–Asian collision zone. *Shadowed columns* reflect intensity of magmatism, defined by estimated volume and age data (see Table 3) of the porphyry stocks in the eastern collision zone (Tang and Luo 1995; Luo et al. 1998; Zhang et al. 1998a; Liang 2002; Hou et al. 2003)

Results

Total Re, ^{187}Re, and ^{187}Os concentrations, and Re–Os ages for molybdenite are reported in Table 2, and are presented in ^{187}Re–^{187}Os isochron diagrams (Fig. 2). The lack of clay intergrowths, the presence of well-constrained ^{187}Re–^{187}Os isochrones with low MSWD, and the similarity to previously reported ages of K–Ar, Rb–Sr, U–Pb dates for host porphyries and hydrothermal minerals (Table 3) indicate that the ages obtained by molybdenite Re–Os data reflect the age of mineralization in the eastern Indo–Asian collision zone.

Yulong

Four samples from the deposit plot along a linear array on the isochron diagram (Fig. 2a). According to the best-fit calculation (Minster et al. 1979), the isochron yields an age of 40.1±1.8 Ma (2σ), using a ^{187}Re decay constant of 1.666×10^{-11}(Smoliar et al. 1996). This age is younger than the ages for pre-ore quartz monzonite (52.0~55.0 Ma) (Table 3; Chen 1983; Ma 1990; Tang and Luo 1995; Hou et al. 2003), but coincident with a zircon sensitive high-mass resolution ion microprobe (SHRIMP) age of 40.9 Ma (Liang 2002). Molybdenites from two other deposits (Malasongduo and Duoxiasongduo) in the Yulong porphyry Cu belt yield similar model ages (35.8±0.4, 36.0± 0.4 Ma), using the less precise isotope dilution-ICP-MS technique (Du et al. 1994). The younger Re–Os ages are within the range defined by K-feldspar K–Ar and zircon U–Pb dates (32.4~40.9 Ma) (see Table 3), but slightly younger than zircon SHRIMP ages (37.1±0.2~37.5± 0.2 Ma) for the host porphyries (Liang 2002).

Machangqing

Eight molybdenite samples from the deposit yielded a weighted Re–Os mean age of 35.6±0.6 Ma (2σ). These molybdenites form an isochron with an age of 35.8±1.6 Ma (2σ) (MSWD=4.1) (Fig. 2b). The Re–Os isochron age is consistent with the age range of 34~36 Ma, obtained by bulk-rock Rb–Sr and zircon SHRIMP dates for the host quartz syenite and granite porphyries (see Table 3; Fu 1996; Luo et al. 1998; Liang 2002), but younger than a K–Ar age of 48.0 Ma for the pre-ore granitic porphyries (Zhang et al. 1998a). This indicates that the molybdenum mineralization is not associated with the early granite phase in the area.

Xifanping

Vein and disseminated molybdenite samples from K-silicate alteration in the host monzonite were analyzed. Five Re–Os molybdenite ages have a weighted Re–Os mean age of 33.1±

Fig. 4 Mineralization age vs tonnage of Cu (**a**) and Au (**b**) of the porphyry-type deposits in the eastern Indo–Asian collision zone. *Y* Yulong, *M* Malasongduo, *D* Duoxiasongduo, *Z* Zhanaga, *Ma* Mangzong, *Mc* Machangqing, *X* Xifanping, *Ya* Yao'an, *B* Beiya, *H* Habo, *C* Chang'an

0.8 Ma (2σ). The ^{187}Re–^{187}Os data for these molybdenites yielded an isochron with an age of 32.1± 1.6 Ma (Fig. 2c). The Re–Os age is slightly younger than the K–Ar ages of 33.5~34.6 Ma for hydrothermal actinolite and biotite in the host monzonitic intrusion (Xu et al. 1997), and much younger than the 51.9 Ma K–Ar age for K-feldspar and the 47.5 Ma ^{40}Ar/^{39}Ar age for amphibole in the pre-ore monzonite porphyries in the area (Fu 1996; Luo et al. 1998).

Discussion

Rhenium concentrations in molybdenite

There is a wide range of Re content (9.4~664.5 ppm) in molybdenite from these three deposits (Table 2). The Re concentrations in molybdenite from the Yulong Cu±Mo deposit (average 444 ppm) and Machangqing Cu–Mo± Au deposits (average 80 ppm) are quite different. The Yulong deposit has a lower Mo grade (0.028%). In contrast, the Machangqing deposit is characterized by a higher Mo grade (0.08%). There appears to be a negative correlation between the Re concentration in molybdenite and the abundance of molybdenite in both deposits. Similar covariation has been recognized between porphyry Cu–Mo and Mo deposits (Giles and Schilling 1972), between non-economic Mo occurrences and Mo deposits (Selby and Creaser 2001), and between less economic vein Mo–Pb and porphyry Mo deposits in the Qinling belt (Stein et al. 1997).

Some researchers attribute different Re concentrations in molybdenite to the temperature/depth of the ore formation (Ishihara 1988) and the polytype of molybdenite (Ayres 1974; Newberry 1979). However, the geological and geochemical similarity between the Yulong and Machangqing deposits suggests that these factors cannot explain the variation in Re concentration (Selby and Creaser 2001). Elevated fO$_2$ is necessary for the partitioning of Mo and Re into the volatile phase (Bernard et al. 1990), but the major factor controlling the concentration of Mo in porphyry Cu–Mo–Au systems may be the fluorine or chlorine content in the hydrothermal fluids (Selby and Creaser 2001). This is because high chlorine content would decrease the amount of Mo transported as hydroxyl complex (Candela and Holland 1984; Keppler and Wyllie 1991). The Yulong deposit is characterized by W- and Bi-bearing minerals (scheelite, bismuthinite) during the porphyry Cu mineralization (Hou et al. 2005), different from the Machangqing deposit. Efficient transport of W and Bi as a chloride complex (Liu et al. 1999) implies high chloride or chlorine content in the Yulong early-stage hydrothermal fluids, as suggested by the high salinity (23~54 wt.% NaCl) of fluid inclusions. This possibly explains the less economic Mo mineralization at Yulong in comparison to the Machangqing deposit.

A much wider variation range for Re concentration (9.4~380.5 ppm) in molybdenite is obtained at Xifanping (Table 2). Such a large variation in Re concentration within one deposit cannot simply be attributed to a variation of fO$_2$ or chlorine content of the porphyry hydrothermal system. Additional factors, such as the crystallization of molybdenite at different stages during the evolution of Cu–Au-bearing fluids or magmas, could be involved.

Mineralization ages and episodes

The three different Re–Os molybdenite ages of 40.1±1.8, 35.8±1.6, and 32.1±1.6 Ma are interpreted as three distinct hydrothermal mineralization events. In the eastern Indo–Asian collision zone, alkali-rich magmatism lasted from 55 to 17 Ma (Hou et al. 2004a), during which three distinct episodes of magmatic emplacement developed in most ore districts (see Table 3), and associated mineralization occurs in the middle–late stages of the porphyry systems. At Yulong, pre-ore quartz monzonitic intrusives yielded ages ranging from 52 to 55 Ma, intra-ore monzogranitic intrusives yielded ages ranging from 37.9 to 41.5 Ma (Table 3), whereas post-ore alkali feldspar granitic intrusives yielded a much younger age of 16.5 Ma (Table 3; Tang and Luo 1995). The correspondence of the Re–Os molybdenite age (40.1± 1.8 Ma) to a zircon U–Pb SHRIMP age (40.9±0.1 Ma) for host monzogranitic porphyries suggests that the Cu–Mo mineralization occurred in the middle stages of the magmatic system at Yulong. Three episodes of magmatism occur in both the Malasongduo and Duoxiasongduo districts (Table 3; Hou et al. 2003), whereas Cu–Mo mineralization with molybdenite Re–Os ages of 35.8~36.0 Ma (Du et al. 1994) is associated with intra-ore monzogranitic porphyries with age of 32.4~41.0 Ma (Table 3). This is also the case at Machangqing, where the pre-ore granite intrusions have a K–Ar age of 48.0 Ma, whereas the mineralized granite and quartz syenite intrusions yielded Rb–Sr isochron ages of 34.0~36.0 Ma (Table 3), overlapping the Re–Os molybdenite age of 35.8±1.6 Ma for the sulfide assemblage. In the Habo and Chang'an Au deposits, the K–Ar and Rb–Sr dates for hydrothermal minerals yielded similar ages ranging from 36.0 to 37.5 Ma (Table 3), also suggesting a similar mineralization event at ~36 Ma.

The latest mineralization event at 32.1±1.6 Ma is suggested by the Re–Os molybdenite age at Xifanping. K-feldspar K–Ar ages and hornblende ^{40}Ar/^{39}Ar ages in pre-ore quartz monzonites range from 51.9 to 47.5 Ma, whereas K–Ar ages of hydrothermal minerals from the K-silicate alteration halo are much younger (33.5 to 34.6 Ma, Table 3; Xu et al. 1997), slightly older than the 32.1± 1.6 Ma Re–Os isochron age for molybdenite. This suggests that the introduction of Cu, Mo, and Au occurred in the late stage of the hydrothermal system (Luo et al. 1998). This mineralization event probably also resulted in the formation of the Yao'an Au deposit, in which hydrothermal biotite from the K-silicate alteration halo in the quartz syenite stock yielded K–Ar ages of 31.0~35.0 Ma (Luo et al. 1998).

The three distinct episodes of Cu–Mo–Au mineralization are related to episodic relaxation of the regional compressional stress, which resulted in a high-level emplacement of felsic magmas (Fig. 3; Hou et al. 2004a). The Cenozoic deformation history indicates that the eastern collision zone was in a transpressional regime since the

Paleocene, and regional extension started at ~20 Ma (Fig. 3, Wang J-H et al. 2001). The earliest magmatism (52± 2.8 Ma) occurred in a transpressional regime, in which large-scale strike-slip faults controlled quartz monzonite and monzogranite intrusions (Hou et al. 2003). The last magmatic event in the early–middle Miocene, with ages ranging from 16.5 to 27.8 Ma, occurred during a transtensional period (Wang J-H et al. 2001), during which large-scale, left-lateral strike-slip movements developed along the Red River shear zone at 23~24 Ma (Tapponnier et al. 1990; Leloup et al. 1995). Three felsic magmatic events peaked at 42±1, 37±1, and 32±1 Ma (Fig. 3), and the associated pull-apart basins were filled with alkaline volcanic lavas of 42.4~37.5 Ma (Zhang and Xie 1997), suggesting their generation during transition from a transpressional to a transtensional regime. This episodic stress relaxation could promote multiple, high-level emplacement of felsic magmas and the exsolution of large volumes of ore-forming fluids, which led to three episodes (40.1±1.8, 35.8±1.6, and 32.1±1.6 Ma) of economically significant mineralization in the eastern Indo–Asian collision zone (Fig. 3).

Correlation between absolute
age and metallic tonnage of deposits

A positive correlation between the absolute age and the metallic tonnage of deposits in the eastern Indo–Asian collision zone has been recognized (see Fig. 4). The positive correlation also appears to hold for individual ore belts, such as the Yulong porphyry Cu belt (see Tables 1 and 3; Fig. 4). It seems that the older the deposits are, the larger the tonnage of metals is (Fig. 4).

The reason for this positive correlation is not clear. Two possibilities could be involved. The one is a prolonged duration of hydrothermal activity, which causes telescoping of the hydrothermal system and overlapping of high-sulfidation mineralization over early-formed porphyry Cu mineralization, thus resulting in large deposits (Padilla Garza et al. 2001; Hou et al. 2005). However, for most porphyry Cu–Mo systems, porphyry emplacement, hydrothermal activity, and sulfide precipitation often occur in a very short time, such as at El Salvador, Chile (0.21~1.02 Ma, Watanabe et al. 1999); Chuquicamata, Chile (2.3 Ma, Ballard et al. 2001); Toquepala, Peru (1 Ma, Clack, 1993); the Andean porphyry system (1~3 Ma, Sillitoe 1988); and the Gangdese porphyry system (0.5~1 Ma, Hou et al. 2004b). Overprinting of epithermal gold mineralization over the porphyry Cu–Mo orebody probably occurred in the Machangqing deposit (Fig. 1d), in which the gold mineralization, structurally controlled by a fracture zone, is associated with strongly altered quartz syenites with 31~32 Ma K–Ar ages (Table 3). However, there are not enough data to determine if both events are gradual and continuous or separated and unrelated. Another possibility is a decrease in the intensity of the felsic magmatic activity with time during the episodic

stress relaxation in the eastern Indo–Asian collisional zone (Fig. 3). The size or volume of the felsic magmas early emplaced at ~42 Ma and the corresponding tonnage of metals (e.g., Yulong) are the largest, whereas the size of felsic magmas emplaced late at ~33 Ma (Fig. 3) and metallic reserves of deposits (e.g., Xifanping) are the smallest. This simple relationship suggests that the larger Cu-bearing magma volumes are the reasons for the larger tonnage.

Conclusions

1. The Re–Os molybdenite ages indicate that there are three distinct episodes (40 Ma, 36 Ma, and 32 Ma) of Cu–Mo–Au mineralization in the eastern Indo–Asian collision zone.
2. Multiple emplacements of magmas and episodic exsolution of ore-forming fluids, caused by episodic stress relaxation, probably led to three episodes of economically significant mineralization in the collision zone.
3. Available age data indicate that there is a positive correlation between the absolute age and the metallic tonnage of Cu–Mo–Au deposits in the collision zone.

References

Ayres D (1974) Distribution and occurrence of some naturally-occurring polytypes of molybdenite in Australia and Papua New Guinea. J Geol Soc Aust 21:273–278

Barra F, Ruiz J, Mathur R, Titley S (2003) A Re–Os study of sulfide minerals from the Bagdad porphyry Cu–Mo deposit, northern Arizona, USA. Miner Depos 38:585–596

Ballard JR, Palin JM, Williams IS, Campbell IH (2001) Two ages of porhyryr intrusion resolved for the super-giant Chuquicamata copper deposit of northern Chile by ELA-ICP-MS and SHRIMP. Geology 29:383–386

Bernard A, Symonds RS, Rose WI (1990) Volatile transport and deposition of Mo, W and Re in high temperature magmatic fluids. Appl Geochem 5:317–326

Cai X-P (1992) Deep-sourced exclave within the Cenozoic alkali porphyry in the West rim of Yangtze Craton and its significance. Chin J Geol 27:183–189 (in Chinese)

Candela PA, Holland HD (1984) The partitioning of copper and molybdenum between silicate melt and aqueous fluids. Geochim Cosmochim Acta 48:373–380

Chen W-M (1983) Relationship of the Yulong porphyry copper deposit with sandstone copper deposits. Contribution to Geology in the Qinghai-Tibet Plateau (13), Geological Publishing House, Beijing (in Chinese)

Clack AH (1993) Are outside porphyry copper deposits either anatomically or environmentally distinctive? Soc Econ Geol Spec Publ 2:213–283

Defant MJ, Drummond MS (1990) Derivation of some modern arc magmas by melting of young subducted lithosphere. Nature 34:662–665

Drummond MS, Defant MJ, Kepezhinskas PK (1996) Petrogenesis of slab-derived trondhjemite-tonalite-dacite/adakite magmas. Trans R Soc Edinb Earth Sci 87:205–215

Du A-D, He H-L, Yin W-N (1994) The study on the analytical methods of Re–Os age for molybdenites. Acta Geol Sin 68:339–346 (in Chinese with English abstract)

Fu D-M (1996) Metallogenic series and regularity of the ferrous and rare, and precious metal ore deposits in the continental orogenic belt, southwestern margins of the Yangtze platform. In: Luo Y-N (ed) Contribution to geology and mineral resources in the continental orogenic belt, southwestern margins of the Yangtze platform. Sichuan Press of Science and Technology, Chengdu, pp 120–129

Ge L-S, Guo X-D, Zhou Y-L, Yang J-H, Li Y-J (2003) Geology and origin of the Yao'an gold deposit, Yunnan, related to alkai-rich magmatism. Geol Resour 10:29–37 (in Chinese)

Giles DL, Schilling JH (1972) Variation in rhenium content of molybdenite. In: 24th International Geological Congress, Montreal Proceedings, vol 10. pp 145–152

Hou Z-Q, Ma H-W, Zaw K, Zhang Y-Q, Wang M-J, Wang Z, Pan G-T, Tang R-L (2003) The Himalayan Yulong porphyry copper belt: produced by large-scale strike-slip faulting at Eastern Tibet. Econ Geol 98:125–145

Hou Z-Q, Zhong D-L, Deng W-M (2004a) A tectonic model for porphyry copper–molybdenum–gold deposits in the eastern Indo–Asian collision zone. Geol China 31:1–14 (in Chinese)

Hou Z-Q, Qu X-M, Wang S-X, Du A-D, Gao Y-F (2004b) Re–Os age for molybdenites from the Gangdese porphyry copper belt in the Tibetan plateau: implication to mineralization duration and geodynamic setting. Sci China 47:221–231

Hou Z-Q, Xie Y-L, Li Y-Q, Xu W-Y, Rui Z-Y (2005) Yulong: a high-sulfidation Cu–Au porphyry copper deposit in the eastern Indo–Asian collision zone, East Tibet. Int Geol Rev (in press)

Huang Z-L, Wang L-K, Zhu C-M (1996) Geochemistry and genesis of the lamprophyres in the Machangqing gold district, Yunnan. Miner Rocks 16:82–89 (in Chinese)

Ishihara S (1988) Rhenium contents of molybdenites in granitoid-series rocks in Japan. Econ Geol 83:1047–1051

Ishihara S, Shibata K, Uchiumi S (1989) K–Ar age of molybdenum mineralization in the east-central Kitakami Mountains, Northern Honshu, Japan: comparison with the Re–Os age. Geochem J 23:85–89

Kay SM, Ramos VA, Marquez M (1993) Evidence in Cerro Pampa volcanic rocks for slab-melting prior to ridge–trench collision in Southern South America. J Geol 101:703–714

Keppler H, Wyllie PJ (1991) Partitioning of Cu, Sn, Mo, W, U, and Th between melt and aqueous fluid in the systems haplogranite-H_2O-HCl and haplogranite-H_2O–HF. Contrib Mineral Petrol 109:139–150

Leloup PH, Lacassin R, Tapponnier R (1995) Kinematics of Tertiary left-lateral shearing at the lithospheric-scale in the Ailao Shan–Red River shear zone (Yunnan, China). Tectonophysics 251:3–84

Li Y-Q, Rui Z-Y, Cheng L-X (1981) Fluid inclusions and mineralization of the Yulong porphyry copper (Mo) deposit. Acta Geol Sin 55:18–23 (Chinese with English abstract)

Liang H-Y (2002) The zircon SHRIMP ages of the Yulong porphyry Cu belt. Report to National Foundation of Natural Science in China (in Chinese)

Liu R-M, Zhao D-H, Huang X-R (1981) Discussion on isotopic ages of acid intrusions in the eastern Tibet. Geol Rev 27:326–332 (in Chinese with English abstract)

Liu Y-M, Wang C-L, Qi Y-Z, Lu H-Z (1999) Metallogenic feature and genetic model of the Shizhuyuan W-polymetallic deposit in China. In Tu G-Z (ed) Super-large deposits in China. Academic Press, Beijing, pp 27–48 (in Chinese)

Luck JM, Allègre CJ (1982) The study of molybdenites through the [187]Re–[187]Os chronometer. Earth Planet Sci Lett 61:291–296

Ludwig KR (2001) Isoplot/Ex version 2.49. A geochronological toolkit for Microsoft Excel. Berkeley Geochronological Center Spec Publ 1a

Luo Y-N, Yu R-L, Hou L-W, Lai S-M, Fu D-M, Chen M-X, Fu X-F, Rao R-B, Zhou S-Q (1998) Longmenshan–Jinpingshan intracontinental orogenic belt. Sichuan Science and Technology Publishing House, Chengdu, p 171 (in Chinese)

Ma H-W (1990) Granitoids and mineralization of the Yulong porphyry copper belt in eastern Tibet. Press of China University of Geosciences, Beijing, p 157 (Chinese with English abstract)

McCandless TE, Ruiz J, Campbell AR (1993) Rhenium behavior in molybdenite in hypogene and near-surface environments: implications for Re–Os geochronology. Geochim Cosmochim Acta 57:889–905

Minster JF, Richard LP, Allègre CJ (1979) [87]Rb–[87]Sr chronology of enstatite meteorites. Earth Planet Sci Lett 44:420–440

Mo X-X, Lu F-X, Shen S-Y, Zhu Q-W, Hou Z-Q, Yang K-H (1993) Sanjiang Tethyan volcanism and related mineralization. Geological Publishing House, Beijing, p 267 (in Chinese with English abstract)

Newberry RJ (1979) Ploytypism in molybdenite (II): relationships between polytypism, ore deposition/alteration stages and rhenium contents. Am Mineral 64:768–775

Padilla Garza RA, Titley SR, Pimentel F (2001) Geology of the Escondida porphyry copper deposit, Antofagast region, Chile. Econ Geol 96:307–324

Peng Z, Watanabe M, Hoshino K, Sueoka S, Yano T, Nishido H (1998) The Machangqing copper–molybdenum deposit, Yunnan, China: an example of Himalayan porphyry-hosted Cu–Mo mineralization. Mineral Petrol 63:95–117

Rui Z-Y, Huang C-K, Qi G-M, Xu J, Zhang M-T (1984) The porphyry Cu (–Mo) deposits in China. Geological Publishing House, Beijing, p 350 (in Chinese with English abstract)

Selby D, Creaser RA (2001) Re–Os geochronology and systematics in molybdenite from the Endako porphyry molybdenum deposit, British Columbia, Canada. Econ Geol 96:197–204

Selby D, Creaser RA, Hart CJR, Rombach CS, Thompson JFH, Smith MT, Bake AA, Goldfarb RJ (2002) Absolute timing of sulfide and gold mineralization: a comparison of Re–Os molybdenite and Ar–Ar mica methods from the Tintina Gold Belt, Alaska. Geology 30:791–794

Shirey SB, Walker RJ (1995) Carius tube digestion for low-blank rhenium–osmium analysis. Anal Chem 67:2136–2141

Sillitoe RH (1988) Epochs of intrusion-related copper mineralization in the Andes. J South Am Earth Sci 1:89–108

Smoliar MI, Walker RJ, Morgan JW (1996) Re–Os ages of group IIA, IIIA, IVA and IVB iron meteorites. Science 271:1099–1102

Stein HJ, Markey RJ, Morgan JW, Du A-D, Sun Y-L (1997) Highly precise and accurate Re–Os ages for molybdenite from the East Qinling molybdenite belt, Shananxi Province, China. Econ Geol 92:827–835

Stein HJ, Sundblad K, Markey RJ, Morgan JW, Motuza G (1998) Re–Os ages for Archean molybdenite and pyrite, Kuittila-Kiviso, Finland and Proterozoic molybdenite, Kabeliai, Lithuania: testing the chronometer in a metamorphic and metasomatic setting. Miner Depos 33:329–345

Suzuki K, Shimizu H, Masuda A (1996) Re–Os dating of molybdenites from ore deposits in Japan: implication for the closure temperature of the Re–Os system for molybdenite and the cooling history of molybdenum ore deposits. Geochim Cosmochim Acta 60:3151–3159

Tapponnier P, Lacassin R, Leloup PH, Scharer U, Zhong D-L, Haiwei W, Liu X-H, Ji S-C, Zhang L-S, Zhong J-Y (1990) The Ailao Shan/Red River metamorphic belt: Tertiary left-lateral shear between Indochina and South China. Nature 343:431–437

Wang D-H, Chen Y-C, Xu J, Yang J-M, Xue C-J, Yan S-H (2001) Major characteristics and mineralized series of the Cenozoic metallogeny in China. Contribution to the 31st International Geological Congress, 264–269 (in Chinese)

Wang J-H, Yin A, Harrison TM (2001) A tectonic model for Cenozoic igneous activities in the eastern Indo–Asian collision zone. Earth Planet Sci Lett 88:123–133

Wang J-Q, Hu R-Z, Sun Y, Lu Y, Li Z-Q (2002) Geochemical studies of K silicate alteration in the Xifanping porphyry Cu deposit. Miner Rocks 22:41–45 (in Chinese)

Watanabe Y, Stein HJ, Morgan JW, Markey RJ (1999) Re–Os geochronology brackets timing and duration of mineralization for the El Salvador porphyry Cu–Mo deposit, Chile (abstract). Geol Soc Am Abs with Prog 31:A30

Xu S-J, Shen W-Z, Wang R-C, Lu J-J, Lin Y-P, Ni P, Luo Y-N, Li L-Z (1997) Characteristics and origin of the Xifanping porphyry copper deposit, Yanyuan County, Sichuan Province. Acta Miner Sin 17:56–62 (in Chinese with English abstract)

Yang J-K, Tang Z-G (1996) Mineralization characteristics and prospective prediction of the Cenozoic porphyry gold deposit in Yunnan Province: exampled by Machangqing gold deposit. Geol Beijing 3:27–31 (in Chinese)

Zhang Y-Q, Xie Y-W (1997) Geochronology and Nd–Sr isotopic features of alkali-rich intrusions in the Ailaoshan-Jinshajiang region. Sci China 27:289–293 (in Chinese)

Zhang Y-Q, Xie Y-W, Qiu H-N, Li X-H, Zhong S-L (1998a) Shoshonitic series: geochemical characteristics of elements for ore-bearing porphyry from Yulong copper ore belt in Eastern Tibet. Earth Sci J China Univ Geosci 23:557–561 (in Chinese)

Zhang Y-Q, Xie Y-W, Qiu H-N, Li X-H, Zhong S-L (1998b) Shoshonitic series: Sr, Nd, and Pb isotopic compositions of ore-bearing porphyry for Yulong copper ore belt in the Eastern Tibet. Sci Geol Sin 33:359–366 (in Chinese with English abstract)